MJSAT

Malaysian Journal of Science and Advanced Technology

journal homepage: https://mjsat.com.my/

Effect of Coriolis Force on the Numerical Estimation of Water Level Elevation Due to a Catastrophic Cyclone along the Coast of Bangladesh

Md. Abdul Al Mohit[1], Md. Towhiduzzaman[*2], and Mst. Rabiba Khatun[1]

[1] *Department of Mathematics, Islamic University, Kushtia-7003, Bangladesh.*
[2] *Department of Electrical & Electronic Engineering (EEE), Uttara University (UU), Dhaka-1230, Bangladesh.*

KEYWORDS

Bangladesh
Coast
Coriolis
FDM
Tide

ARTICLE HISTORY

Received 17 August 2022
Received in revised form 23 August 2022
Accepted 26 August 2022
Available online 27 August 2022

ABSTRACT

A two-dimensional vertically integrated shallow water equation in the Cartesian coordinate model is used to estimate the water level considering the impact of Coriolis force. The shallow water model equation was discretized by a finite difference method (FDM). Consider the forwarding of time and central space as a moderator of this discretization. The model approximates coastal boundaries, small islands, small rivers and complex tributaries by an accurate stair step representation. The model equations are solved by a static semi-implicit finite difference technique where a structured Arakawa C-grid system is used as the condition. A one-way nested scheme technique is used to incorporate complex land-sea interfaces such as small offshore islands and water depths with sufficient accuracy as well as decreasing the computational cost. A stable tidal condition was created by applying M2 tidal forcing with the largest tide along the southern open boundary of the Bay of Bengal. The model uses the Coriolis force as an external force that can affect water buoyancy. The main task is to analyse the effect of Coriolis force on water buoyancy. The described model was applied to simulate sea-surface elevation associated with the severe cyclone in April 1991 that strike on the east coast of Bangladesh. We have found a significant impact of Coriolis force on surge height. However, the model gives an accurate numerical estimate of surge height.

1. INTRODUCTION

Bangladesh is a low-lying country in south Asia which is situated at the northern tip of the Bay of Bengal. The coast of Bangladesh is affected by various environmental problems. Storm surge is one of them which causes a tremendous loss of lives and properties every year. It is caused by a combination of wind and low atmospheric pressure. An increasing number of tropical cyclones associated with surge always cause a great loss of many lives and properties along the region of interest. Cyclones in November 1970, 1985, April 1991, 1997, SIDR 2007, and AILA 2009 caused a lot of death tools [1]. Many analyses on prediction of surge due to tropical storms have been made for the Bay of Bengal region covering the coastal area of Bangladesh and the east coast of India [1]–[9]. Though a considerable number of studies have been done for the coast of Bangladesh, none of them can be analysed the effect of Coriolis force on storm surge estimation. The Coriolis effect refers to the apparent deflection of objects in motion in physics. The motion of objects is described in this case relative to a rotational context frame. In a clockwise rotational context frame, the object's direction of motion is deviated to the left. And in case of counter clockwise rotation, the deviation occurs to the right. The Coriolis force is proportional to the rate of rotation and the centrifugal force is proportional to the square of the rate of rotation. The Coriolis force acts perpendicular to its axis of rotation and in the direction of the motion of the object in the rotating frame and is proportional to the motion of the object in the rotating frame. The centripetal force acts outward along the radius and is proportional to the distance of the object from the axis of rotation [10]. These additional forces are called passive forces,

*Corresponding author:
E-mail address: Md. Towhiduzzaman < towhid.math.iu@gmail.com >.

imaginary or pseudo forces. These forces play a role in the application of Newton's laws to any structural system. These are correction factors that do not exist in balanced dynamic or static context structures [11]. Some of the researchers focus on the Coriolis force and its associated surge effect [12]. He explains the Coriolis force effect on storm surge estimation, but he did not include its full effects on the topography and typhoon changes. In this study, we have investigated the surge height considering different Coriolis forces.

It is seen from the literature point of view that water levels associated with storm surges may be influenced by Coriolis force. An investigation of storm surge forecasting models including Coriolis force to predict the water level accurately which can contribute to improving the warning system and definitely used in real time prediction of the water levels at different locations along the coastal belt of Bangladesh. The present study is an analysis of the estimation of water level including Coriolis parameter based on the Cartesian coordinate system of incorporating the complexity of the coast of Bangladesh.

In this study, we used a two-dimensional shallow water equation to generate the numerical simulation results of storm surge considering different changes of Coriolis force. We believe that the results obtained in our research are very acceptable because our model simulation results make good agreement with the observed result. In the next sections, the details of the subject matter of the research are discussed in stages.

2. DATA MATERIAL AND METHODS

2.1. Study Area

Bangladesh is a delta-like sovereign country in South Asia whose official name is the People's Republic of Bangladesh. Geographically, Bangladesh is bordered by Myanmar to the southeast, India to the west, north and east, and the Bay of Bengal to the south. In this study, our main focus of our research is the disaster-prone coastal region of Bangladesh.

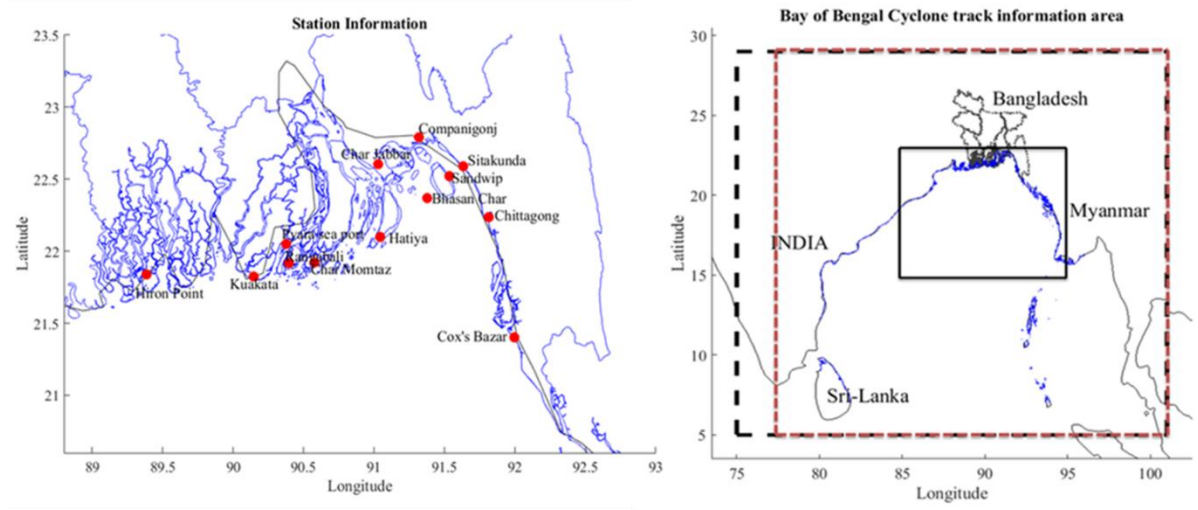

Fig. 1. Study Area with tidal location

Geographically, Bangladesh is located at the northern end of the Bay of Bengal (see, Fig. 1) between 88 to 92 degrees East longitude and 20 to 26 degrees North latitude. If we talk about its surrounding countries, it is surrounded by the landmasses of India, Myanmar and the Bay of Bengal in the south. About 700 rivers flow through Bangladesh with small and large tributaries which create many islands in coastal regions. While this study focuses on coastal islands, special attention is paid to certain regions and islands (like Hatia, Bhola, etc.).

2.2. Model Equation

In this study for the numerical analysis, we considered a rectangular Cartesian coordinate system where the Earth's surface curvature is assumed to be zero along a horizontal XY-plane and an upward z-axis. If the ratio of the horizontal length scale to the vertical length scale is greater than zero, the z component of the momentum equation can be approximated by the hydrostatic equation. Furthermore, if the seawater density variation is negligible, the continuity equation reduces to non-divergence of the velocity. Ignoring this approximation and molecular viscosity, we obtain the basic shallow water equations. Neglecting this shallow water approximation and molecular viscosity, an initial set of shallow water equations [2] is given

$$\frac{\partial u}{\partial t} + u\frac{\partial u}{\partial x} + v\frac{\partial u}{\partial y} + w\frac{\partial u}{\partial z} - fv = -\frac{1}{\rho}\frac{\partial p}{\partial x} \quad (1)$$

$$\frac{\partial v}{\partial t} + u\frac{\partial v}{\partial x} + v\frac{\partial v}{\partial y} + w\frac{\partial v}{\partial z} + fu = -\frac{1}{\rho}\frac{\partial p}{\partial y} \quad (2)$$

$$\frac{\partial p}{\partial z} = -\rho g \quad (3)$$

$$\frac{\partial u}{\partial x} + \frac{\partial v}{\partial y} + \frac{\partial w}{\partial z} = 0 \quad (4)$$

where u, v, w are the instantaneous components of velocity in the directions of *x*, *y*, and *z* respectively; t is the time; p is the pressure; ρ the density of the sea water supposed homogenous and incompressible; $f = 2\Omega \sin\varphi$ the Coriolis parameter, where Ω is the angular speed of the Earth rotation and φ is the latitude of the place of interest; g the acceleration

due to gravity. After applying average procedure, vertical integration process simplifies the equation we may get the basic shallow water model equation as

$$\frac{\partial \zeta}{\partial t}+\frac{\partial \tilde{u}}{\partial x}+\frac{\partial \tilde{v}}{\partial y}=0 \quad (5)$$

$$\frac{\partial \tilde{u}}{\partial t}+\frac{\partial(u\tilde{u})}{\partial x}+\frac{\partial(v\tilde{u})}{\partial y}-f\tilde{v}=-g(\zeta+h)\frac{\partial \zeta}{\partial x}+\frac{T_x}{\rho}-\frac{C_f\,\tilde{u}\sqrt{(u^2+v^2)}}{\zeta+h} \quad (6)$$

$$\frac{\partial \tilde{v}}{\partial t}+\frac{\partial(u\tilde{v})}{\partial x}+\frac{\partial(v\tilde{v})}{\partial y}+f\tilde{u}=-g(\zeta+h)\frac{\partial \zeta}{\partial x}+\frac{T_y}{\rho}-\frac{C_f\,\tilde{v}\sqrt{(u^2+v^2)}}{\zeta+h} \quad (7)$$

$$\text{Where } (\tilde{u},\tilde{v})=(\zeta+h)(u,v) \quad (8)$$

In the above equations, u and v in the bottom stress terms have been replaced in order to solve the equations numerically in a semi-implicit manner.

2.3. Model Setup

2.3.1. Setup boundary conditions

The lateral boundary of the sea area must satisfy appropriate conditions that always work properly during the model simulation under consideration. But since our study area has an ocean to the south, we can consider three-dimensional boundary conditions. Considering some ocean dynamics, a radiation-type boundary condition is applied to the southerly gap region. Such boundary conditions can help external forces enter the open. Therefore, the main boundary conditions are assumed as follows.

$$\text{At the west boundary: } v+\left(\frac{g}{h}\right)^{\frac{1}{2}}\zeta=0 \quad (9)$$

$$\text{At the east boundary: } v-\left(\frac{g}{h}\right)^{\frac{1}{2}}\zeta=0 \quad (10)$$

At the south boundary:

$$u-\left(\frac{g}{h}\right)^{\frac{1}{2}}\zeta=-2\left(\frac{g}{h}\right)^{\frac{1}{2}} a\,sin\,sin\,\left(\frac{2\pi t}{T}+\varphi\right) \quad (11)$$

2.3.2. Determination of the forcing terms

In general, the horizontal gradient of atmospheric pressure is negligible compared to the length scale of a mesoscale ocean model. On the other hand, during a storm, the factor is not negligible, but the main mechanism in generating the wave amplitude is the tangential stress due to the strong winds associated with the storm. Therefore, to calculate tides, waves and their interactions, atmospheric pressure gradients and tangential factors can be neglected. The Coriolis force can be determined by knowing the latitudinal location of the area. Also, the effect of the changing Coriolis force can be analysed. Generally speaking, wind pressure is measured in terms of the wind field associated with the storm. This is often done by the conventional quadratic law:

$$T_x=C_D\rho_a(u_a^2+v_a^2)^{\frac{1}{2}} \text{ and } T_y=C_D\rho_a(u_a^2+v_a^2)^{\frac{1}{2}} \quad (12)$$

Where C_D is known as the drag coefficient, which is also assumed to be constant in our model. For the Bay of Bengal region, the wind field associated with a storm is not available from the Bangladesh Meteorological Department (BMD). Rather, the information is available in terms of the maximum sustained wind velocity and the corresponding radial distance from the eye of the storm and the difference of the atmospheric pressure between the eye and periphery. The circulatory wind field is at that point created by different observational formulae. As in [5], for the Bay of Bengal region most frequently used formula is due to [13], which is given by

$$V_a=\begin{cases}V_0\sqrt{(r_a/R)^3} & for\ all \quad r_a\le R\\ V_0\sqrt{(R/r_a)^3} & for\ all \quad r_a>R\end{cases}, \quad (13)$$

where V_0 is the maximum sustained wind at the radial distance R and r_a is the radial distance at which the wind field is desired. The x and y components (u_a, v_a) of the wind field are derived from V_a given by the above empirical formula.

2.3.3. Setup nested scheme

In this study, it can be seen that the model area is large enough to properly include island boundaries and coastlines in our numerical scheme, so we include the specific area of our study in a much smaller mesh size. Several are real for the mesh size to be a small problem, which has been observed in many studies recently. The problems are

(i) The result will be correct. If the discussion area is defined by small meshes, the number of grid points for these small meshes is greatly increased. This requires large storage facilities in computer memory that cannot be accommodated with small laboratory computers.

(ii) The Courant-Friedrichs-Lewy (CFL) stability criteria must be ensured at the grid points because the size of each grid point and the time step of the arithmetic process determine the stability.

So, according to [14], the time step Δt must be related to the mesh size, Δx (or Δy), and ocean depth, h, by the relation

$$\Delta t\le\frac{\Delta x}{\sqrt{2gh}} \quad (14)$$

Taking the above two facts into consideration, a high-resolution numerical scheme (FMS) is nested in a coarse mesh scheme (CMS) for the desired region. Further, to consider the densely populated low-lying large and small offshore islands between Barisal and Chittagong and to accurately incorporate land dynamics in the numerical model, a very fine mesh scheme (VFMS) is nested in the FMS (See, Fig. 2). The grid size along the north-south direction (along the x-axis) is Δx = 15.08 km and along the east-west direction (along the y-axis) is Δy = 17.52 km. The computational xy-plane has 60x61 grid points with FMS 21^0-15^0N which covers the area between 15^0N to 23^0 N latitude and 89^0 E to 92^0 E longitude. The scheme area includes the study area and almost all offshore islands.

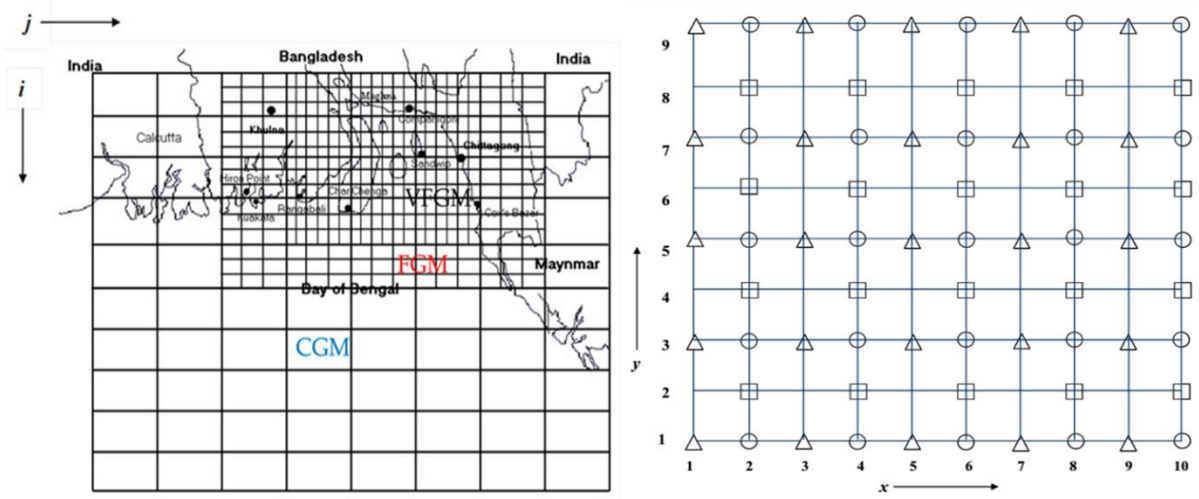

Fig. 2. Numerical schemed area and gridding system

The grid size along the north-south direction (along the x-axis) is Δx = 2.15 km and along the east-west direction (along the y-axis) is Δy = 3.29 km. The computational xy-plane has 92x95 grid points. VFMS covers the area between 21.77^0 N to 23^0 N latitude and 90.40^0 E to 92^0 E longitude. The mesh size along the north-south direction (along the x-axis) is Δx = 720.73 m and along the east-west direction (along the y-axis) is Δy = 1142.39 m. The computational xy-plane has 190×145 grid points. Details of various schemes are also presented in tabular form. Table 1.1 shows the Domains, grid spacing, and number of computational points of different schemes. So we can say, a grid is a small-scale geometric shape covering the physical domain, whose purpose is to identify discrete volumes or elements where conservation laws can be applied.

Table 1.1 Computational points of different schemes considering domains and their grid spacing

Scheme	Domain	Grid spacing along x axis (km)	Grid spacing along y axis (km)	Number of Computational points
CMS	15^0 -23^0 N, 85^0 - 95^0 E	15.08	17.52	60×61
FMS	21^0-15′- 23^0 N, 89^0 E to 92^0 E	2.15	3.29	192×95
VFMS	21.77^0 -23^0 N 90.40^0 - 92^0 E	0.72073	1.14239	190×145

2.3.4. Discretized form of model equation

The governing equation (5) to (7) and the boundary conditions (9) to (11) are discretized by finite-difference technique (forward in time and central in space) and are solved by conditionally stable semi-implicit methods using a staggered grid system. So, the finite-difference method is as follows

$$\zeta_{i,j}^{k+1} = \zeta_{i,j}^{k} - \Delta t[TL1 + TL2] \tag{15}$$

$$\tilde{u}_{i,j}^{k+1} = \frac{\tilde{u}_{i,j}^{k} - \Delta t(TL1+TL2+TL3)+\Delta t(TR1+TR2)}{(1+\Delta t.FR3)} \tag{16}$$

$$\tilde{v}_{i,j}^{k+1} = \frac{\tilde{v}_{i,j}^{k} - \Delta t(TL1+TL2+TL3)+\Delta t(TR1+TR2)}{(1+\Delta t.FR3)} \tag{17}$$

Consider, $\zeta_{i,j}^{k+1}$ in equation (15) is computed at i = 2, 4, 6, … , M – 2. and j = 3, 5, 7, … , N -2. $\tilde{u}_{i,j}^{k+1}$ in equation (14) is computed at i = 3, 5, 7, … , M –1 and j = 3, 5, 7, … , N –2 and $\tilde{v}_{i,j}^{k+1}$ equation (17) is computed at i = 2, 4, 6,....., M –2 and j = 2, 4, 6, … , N –1. In the similar case the discretize form of the boundary conditions are

$$\zeta_{i,1}^{k+1} = -\zeta_{i,3}^{k+1} - 2\sqrt{\frac{h_{i,2}}{g}}V_{i,2}^{k} \tag{18}$$

$$\zeta_{i,N}^{k+1} = -\zeta_{i,N-2}^{k+1} - 2\sqrt{\frac{h_{i,N-1}}{g}}V_{i,N-1}^{k} \tag{19}$$

$$\zeta_{M,j}^{k+1} = -\zeta_{M-2,j}^{k+1} + 2\sqrt{\frac{h_{M-1,j}}{g}}U_{M-1,j}^{k} + 4a\sin\left(\frac{2\pi k\Delta t}{T} + \varphi\right) \tag{20}$$

where, i = 2, 4, 6, … , M –2. and j = 1, 3, 5, 7, … , N.

2.3.5. Numerical procedure

A stable tidal regime was generated over the model domain by first applying the strongest tidal component near the open boundary, the semidiurnal principal lunar tide. The period of tidal oscillation is taken as 12.4 hours. It is noted here that the period of tidal oscillation in the region of interest is not exactly periodic but the average period is found to be about 12.4 hours [9]. The initial values of amplitude and phase relative to the component are determined through equation (19) along the southern open boundary of the CMS following [15]. Then using the atmospheric pressure gradient force and constants involving a component from the initial state of rest

in the absence of wind pressure, a stable tidal regime was achieved after 4 tidal cycles. But the generation of a pure tidal condition depends on the exact value of a and we have followed the technique of [9] for precise specification of the values of the constant. Its initial values are taken as zero to represent a cold start and from this time, a stable tidal system develops in the analysis area. The tidal regime at the start of the model provides the initial state of the ocean at the time of the model, and after a certain period, tidal effects are obtained in coastal areas. The time step is taken as 60 seconds which ensures the Courant-Friedrichs-Lewy (CFL) criterion for stability of the numerical schemes.

3. RESULTS

We computed our results at some representative coastal and island locations of Bangladesh for a specific major storm that hit the coast of Bangladesh. Records show that April 1991 was the most severe cyclonic storm having maximum wind speed 235 km/h.

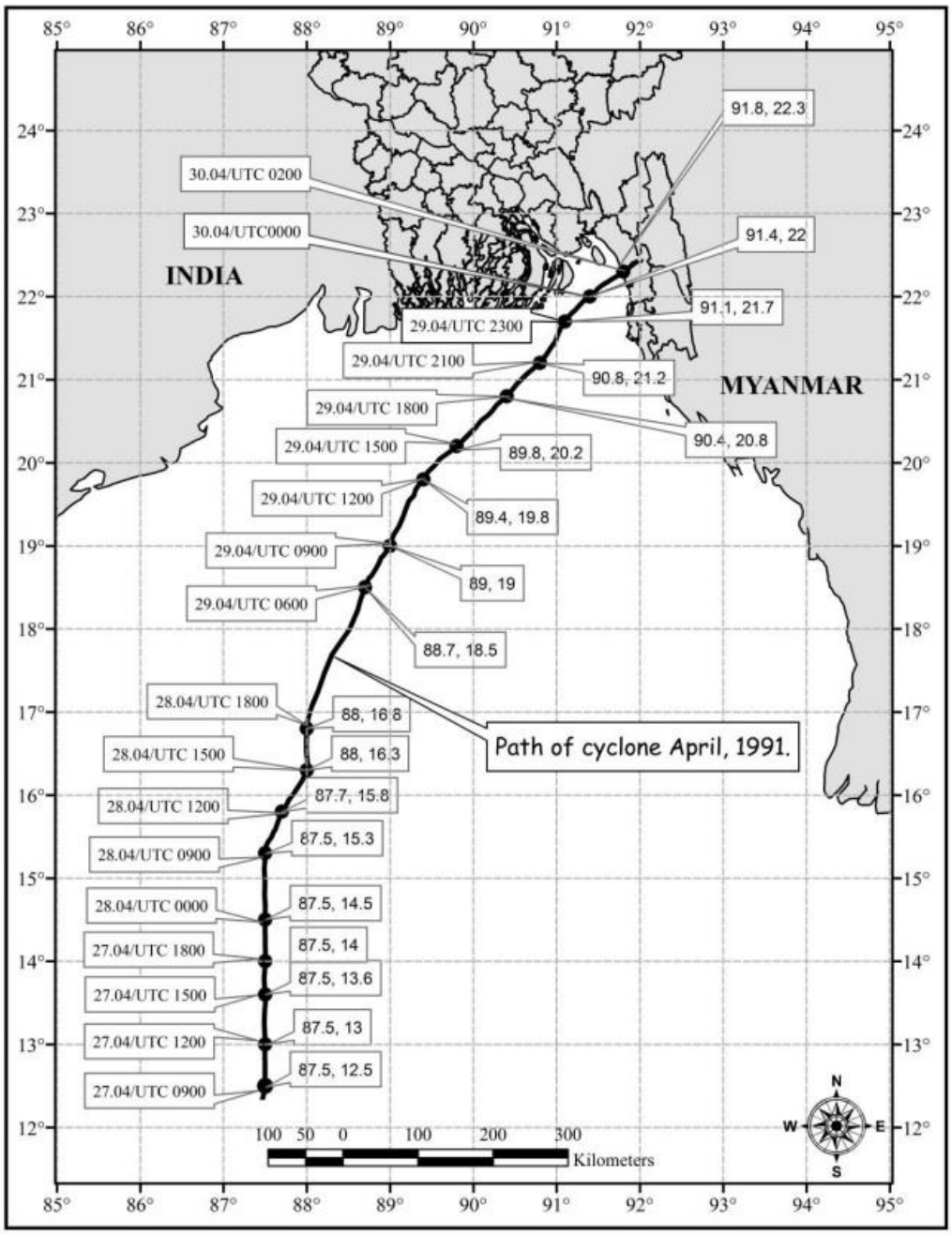

Fig. 3. Schematic track with eye location of cyclone, April 1991

To discuss the results, history of the storm is necessary. The history of the storm is briefly described in the following subsection. The most severe cyclonic storm of the last century hit the coast of Bangladesh on the early morning of April 30, 1991. The cyclone April 1991 was first detected as a depression (wind speed < 62 km/h) on 23rd April in the satellite picture taken at the Space Research and Remote Sensing Organization (SPARRSO) from NOAA-II and GMS-4 satellites. The depression was located at 10.0^0 N latitude and 89.0^0E longitude at 0900 Bangladesh Standard Time (BST) in the morning of April 25. The system intensified into a deep depression in the evening and very quickly turned into a cyclonic storm at midnight of April 25. The maximum sustained wind speed was 65-87 km/h, having a central pressure of 996 mbar.

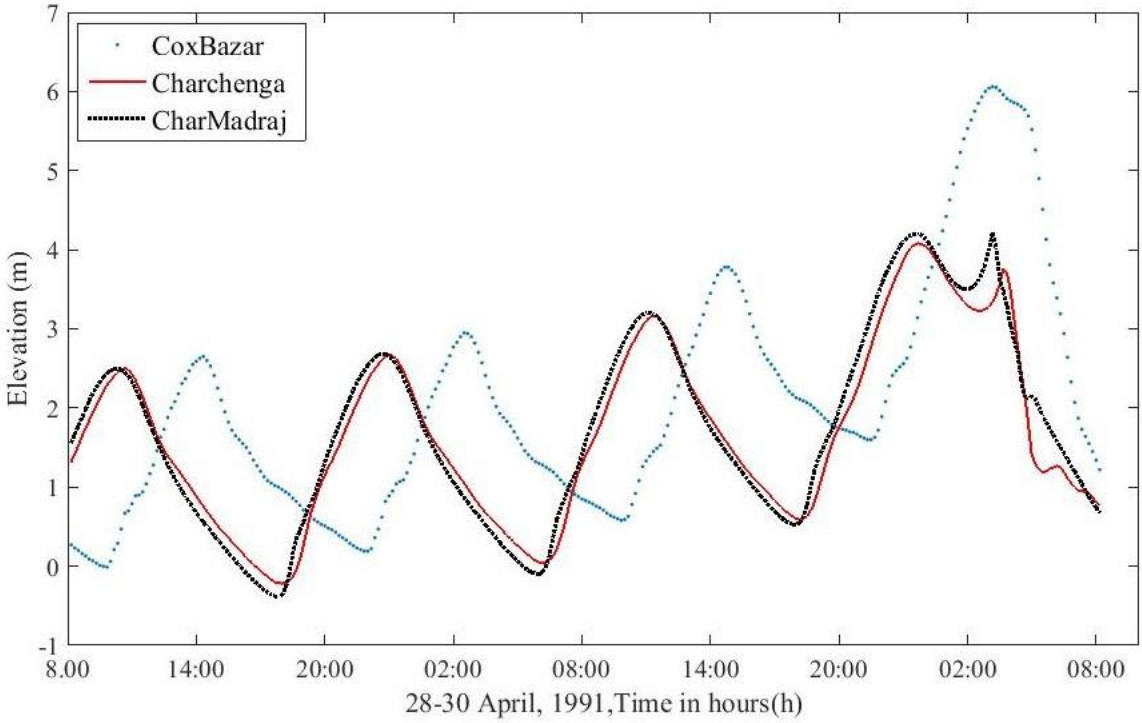

Fig. 4. Water levels with respect to the mean sea level due to tide, surge and the non-linear interaction of tide and surge associated with the storm April 1991 along the coast of Bangladesh considering the actual Coriolis force

It maintained this intensity until 1500 BST on 27 April when it became a severe cyclonic storm. The maximum wind velocity was 90-115 km/h, having 990 mbar as the central pressure. On the same day at midnight, it turned into a storm with a core of hurricane wind that had wind speeds of more than 130 km/h. From 28 April, it started moving northeastward and finally crossed the coast north of Chittagong port on the Noakhali coast in the early hours of 30 April (0600 BST) (Fig. 3) We have used cyclone information in our model to compute the surge height and compare the result with observed data. For this study, we have collected cyclone information from the Bangladesh Meteorological Department (BMD). After running the model, we get the result that is shown in Fig. 4. From this figure, we have found that the surge height near the Cox bazar, Charchanga and Charmadraj varies from 4 to 6 m. We have also found that the surge height around the coast area is 3.5 to 6.2 m. [16] shows 4-6 meter average surge along this region due to the cyclone 1991. Before we run the model, we have set up M2 tide in the open boundary [17]. After that we found the tidal range near the Cox bazar is -0.5 to 2.1 meter (see, Fig. 5). In our model, we have made a non-linear interaction with tide and surge. For all the situations, we consider the actual Coriolis force for simulation. To find the influence of Coriolis force on the surge estimation we consider different values of Coriolis force.

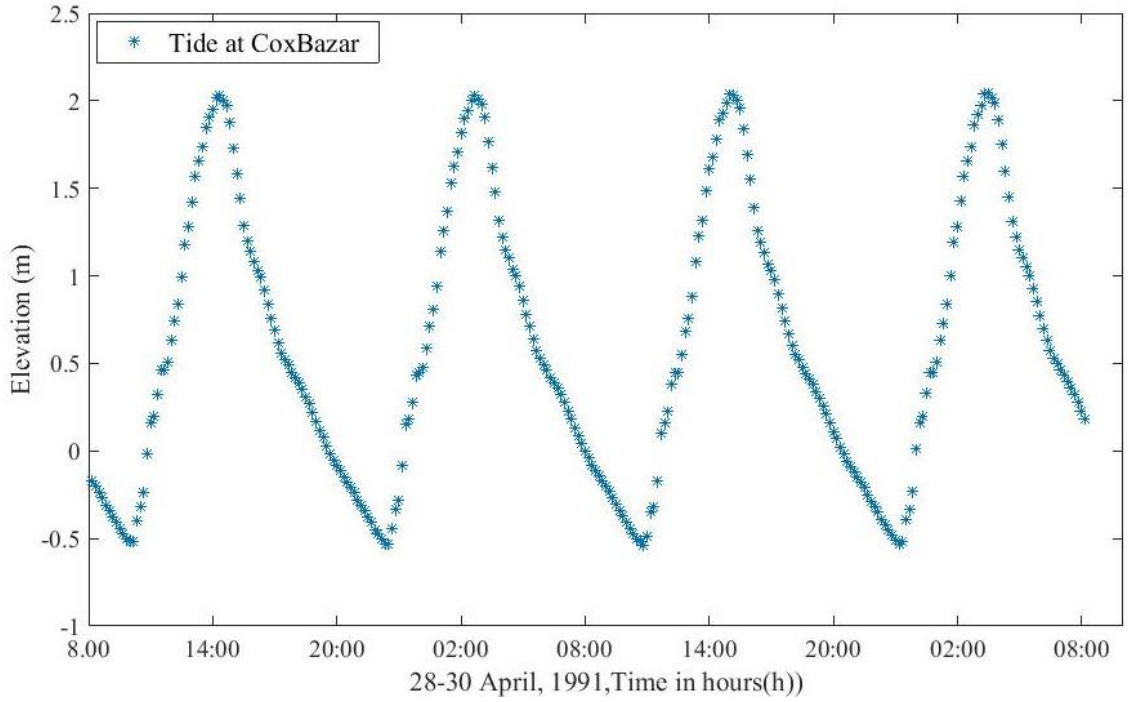

Fig. 5. Water levels with respect to the mean sea level due to tide along the coast of Bangladesh during the storm April 1991

We have considered the Coriolis value for the Bay of Bengal region $2.6x10^{-3}$ as the actual Coriolis force value. Then we increase 25% of the actual Coriolis force. After consideration of the increasing Coriolis force, we run the model again. In the similar way, we have run the model again for decreasing value. Fig. 6 shows the comparison of water level for the different Coriolis value due to a catastrophic cyclone 1991.

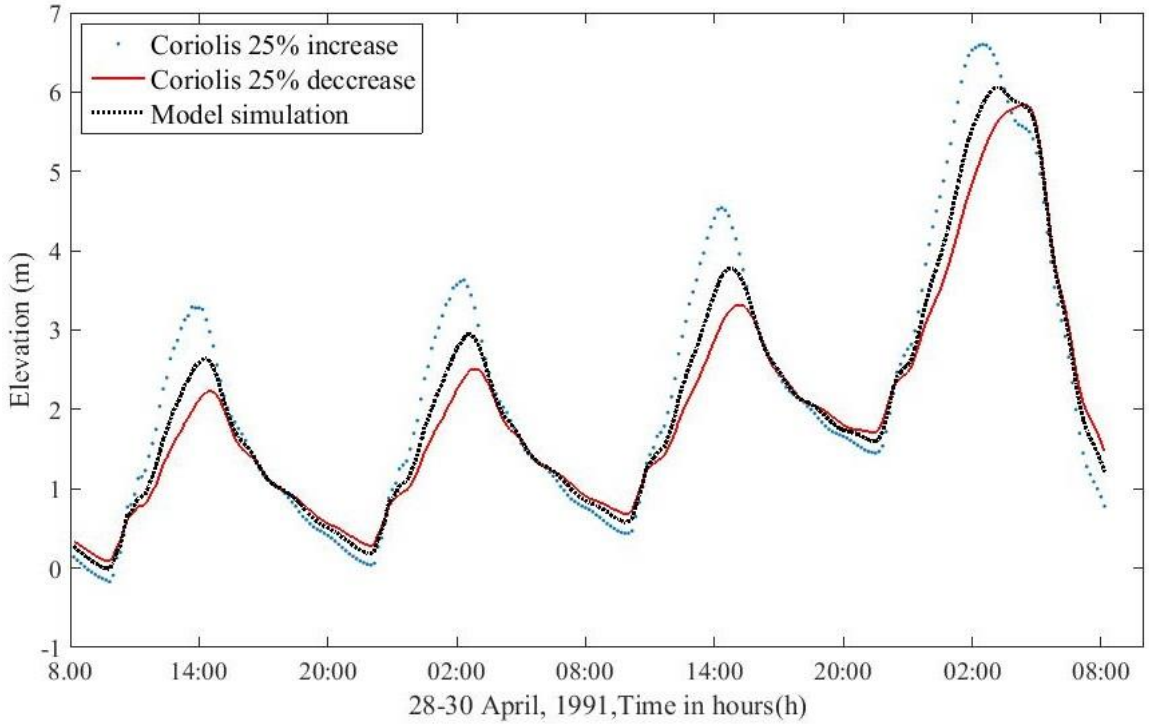

Fig. 6. Water levels with respect to the different Coriolis effect

From the above figure, we found that the changes of water label due to change of the Coriolis value. Thus, it is cleared that the Coriolis force has some effect on the surge height.

4. DISCUSSIONS

In this study, changes in storm surges due to variations in the Coriolis force were observed. Where it has been observed that variations in the Coriolis force cause changes in storm buoyancy. Before examining these issues, we review our model simulation results for the deadly 1991 cyclone. The simulation results are given in Fig. 4 above. In the storm of 1991, the highest inundation was seen in Cox's Bazar and its surrounding areas. However, when the storm of 1991 hit, there was a very large surge due to the tidal effect, which caused a lot of damage to human life and property.

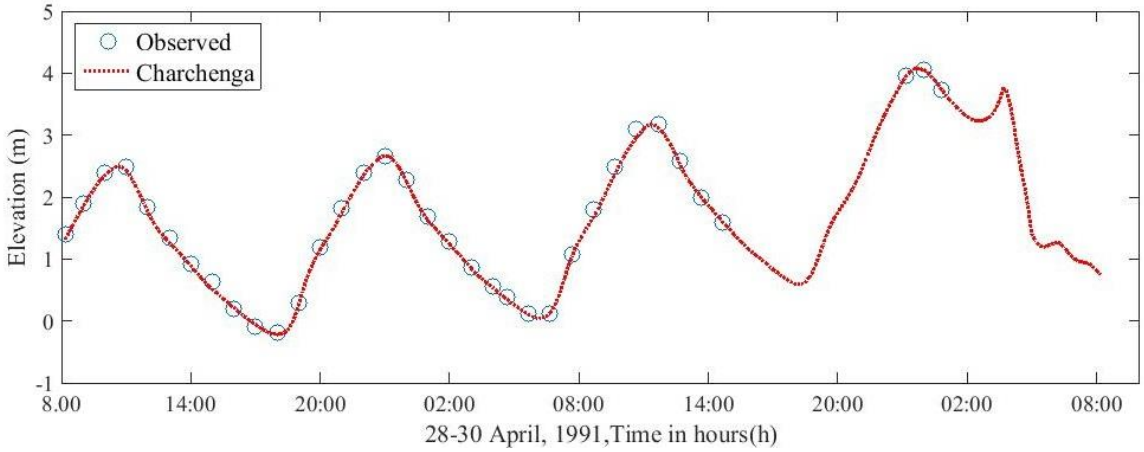

Fig. 7. Comparison of computed water levels with observed data

We therefore compare simulation results and observational data to determine whether the 1991 storm surge measurements are accurate or not. We find good agreement between our model simulation results and observational results. At Charchenga, a sub-district of Bangladesh, we see a good match between the simulation results and the observation results. However, due to non-availability of digital gauges and adverse weather conditions, tide data was not available at all time. After matching the results, we try to see the effect of Coriolis force. To that end, we change the value of the Coriolis force. Values are changed by 25% above and below the original value and watch the tide change for that changing mana. It can be seen that the required change in the Coriolis force value 25 decrease or increase is not obtained. It can be seen that when the value of Coriolis force is high, the model does not give accurate results. However, it is observed from this research that the effect of Coriolis force is small, but it has a significant role in surge height.

5. CONCLUSION

In this study, the simulation of storm surges has been carried out including different Coriolis forces. Considering different values of Coriolis force to the prediction of sea surface elevations along the coastal area of Bangladesh due to the interaction of tide and surge associated with a storm. The model is based on a semi-implicit finite difference method (FDM) with proper stair step representation. Nested grid techniques have been exercised. The model simulations results are found to be better in comparison with observed and reported results obtained through various investigators. Overall water levels can be found to be influenced by Coriolis force.

ACKNOWLEDGMENTS

The first author acknowledges receipt of a project from the University Grant Commission (UGC) of Bangladesh. The first author would like to express his gratitude to the Government of Bangladesh for the project fund during the research period. We would also like to thank the staff of the Department of Mathematics (Islamic University, Bangladesh) for their endless support of laboratory facilities.

CONFLICT INTEREST

The authors declare no competing financial or personal interests that may appear and influence the work reported in this paper.

REFERENCES

[1] M. M. Rahman, A. Hoque, G. C. Paul, and M. J. Alam, "Nested Numerical Schemes to Incorporate Bending Coastline and Islands of Bangladesh and Prediction of Water Levels due to Surge," *Asian J. Math. Stat.*, vol. 4, no. 1, pp. 21–32, Dec. 2010, doi: 10.3923/AJMS.2011.21.32.

[2] M. A. Al Mohit, M. Yamashiro, N. Hashimoto, M. B. Mia, Y. Ide, and M. Kodama, "Impact assessment of a major river basin in Bangladesh on storm surge simulation," *J. Mar. Sci. Eng.*, vol. 6, no. 3, p. 99, Aug. 2018, doi: 10.3390/JMSE6030099.

[3] M. A. Al Mohit and M. Towhiduzzaman, "A numerical estimate of water level elevation due to a cyclone associated with a different landfall angle," *Sains Tanah*, vol. 19, no. 1, pp. 33–41, Mar. 2022, doi: 10.20961/stjssa.v19i1.56600.

[4] A. A. Mohit, Y. Ide, M. Yamashiro, and N. Hashimoto, "A comparative study of two different numerical methods on storm surge," *Proc. 9th Int. Conf. APAC 2017*, no. 213039, pp. 163–174, 2018, doi: 10.1142/9789813233812_0016.

[5] G. C. Paul and A. I. M. Ismail, "Numerical modeling of storm surges with air bubble effects along the coast of Bangladesh," *Ocean Eng.*, vol. 42, pp. 188–194, Mar. 2012, doi: 10.1016/j.oceaneng.2012.01.006.

[6] G. C. Paul and A. I. M. Ismail, "Tide-surge interaction model including air bubble effects for the coast of Bangladesh," *J. Franklin Inst.*, vol. 349, no. 8, pp. 2530–2546, Oct. 2012, doi: 10.1016/j.jfranklin.2012.08.003.

[7] G. C. Paul and A. I. M. Ismail, "Contribution of offshore islands in the prediction of water levels due to tide-surge interaction for the coastal region of Bangladesh," *Nat. Hazards*, vol. 65, no. 1, pp. 13–25, Aug. 2013, doi: 10.1007/s11069-012-0341-z.

[8] A. S. M. Alauddin Al Azad *et al.*, "Impact of tidal phase on inundation and thrust force due to storm surge," *J. Mar. Sci. Eng.*, vol. 6, no. 4, p. 110, Sep. 2018, doi: 10.3390/jmse6040110.

[9] M. Deb and C. M. Ferreira, "Simulation of cyclone-induced storm surges in the low-lying delta of Bangladesh using coupled hydrodynamic and wave model (SWAN + ADCIRC)," *J. Flood Risk Manag.*, vol. 11, pp. S750–S765, 2018, doi: 10.1111/jfr3.12254.

[10] W. Gong, G. Zhang, L. Yuan, H. Zhang, and L. Zhu, "Effect of the Coriolis Force on Salt Dynamics in Convergent Partially Mixed Estuaries," *J. Geophys. Res. Ocean.*, vol. 126, no. 12, p. e2021JC017391, Dec. 2021, doi: 10.1029/2021JC017391.

[11] J. B. Arnell, "Toward a Conceptual Approach to the Coriolis Force: Cataloging Intuitive Knowledge Elements in Intermediate Physics Learners," *All Grad. Theses Diss.*, Aug. 2022, doi: https://doi.org/10.26076/5615-1eb5.

[12] S. Y. Kim, Y. Matsumi, T. Yasuda, and H. Mase, "Effects of Coriolis force on storm surge along west coast of Japan sea," *Proceedings of the International Offshore and Polar Engineering Conference*. OnePetro, pp. 414–421, Jun. 19, 2011.

[13] G. C. Paul, M. M. Murshed, M. R. Haque, M. M. Rahman, and A. Hoque, "Development of a cylindrical polar coordinates shallow water storm surge model for the coast of Bangladesh," *J. Coast. Conserv.*, vol. 21, no. 6, pp. 951–966, Oct. 2017, doi: 10.1007/s11852-017-0565-x.

[14] M. M. Rahman, G. C. Paul, and A. Hoque, "Nested numerical scheme in a polar coordinate shallow water model for the coast of Bangladesh," *J. Coast. Conserv.*, vol. 17, no. 1, pp. 37–47, 2013, doi: 10.1007/s11852-012-0216-1.

[15] R. A. Flather and K. P. Hubbert, "Tide and Surge Models for Shallow Water — Morecambe Bay Revisited," *Model. Mar. Syst.*, pp. 135–166, Jan. 2018, doi: 10.1201/9781351074698-7.

[16] M. A. Hussain and Y. Tajima, "Numerical investigation of surge–tide interactions in the Bay of Bengal along the Bangladesh coast," *Nat. Hazards*, vol. 86, no. 2, pp. 669–694, Dec. 2017, doi: 10.1007/s11069-016-2711-4.

[17] L. Rose and P. K. Bhaskaran, "Tidal variations associated with sea level changes in the Northern Bay of Bengal," *Estuar. Coast. Shelf Sci.*, vol. 272, p. 107881, Aug. 2022, doi: 10.1016/j.ecss.2022.107881.